

# Spin-polarized current generated by carbon chain and finite nanotube

Y. D. Guo, X. H. Yan,<sup>a)</sup> and Y. Xiao

*College of Science, Nanjing University of Aeronautics and Astronautics, Nanjing 210016, People's Republic of China*

(Received 22 June 2010; accepted 2 October 2010; published online 19 November 2010)

Inspired by recent progress of experimental fabrication of carbon structure [Borrmert *et al.*, Phys. Rev. B **81**, 085439 (2010)], we proposed a scheme to generate spin-polarized current based on an all-carbon system consisting of carbon nanotube and chain. The transmission spectra are calculated based on density functional theory combined with nonequilibrium Green's function method. It is found that the spin-polarized current can be achieved in the proposed system by partial contact between nanotube and chain, without using the dopants, ferromagnetic electrodes, and external electric field. Moreover, our results show that the device containing carbon nanotubes with large length and diameter can produce the current with 100% spin polarization, which is essential for spintronic devices. Physical mechanisms and the comparison with the results of graphene are also discussed. © 2010 American Institute of Physics. [doi:10.1063/1.3510537]

## I. INTRODUCTION

Spintronics is a promising field for information processing, storage and many other applications, and in recent years, much effort has been devoted into it.<sup>1–5</sup> One of the key points in this area is the manipulation of the spin polarization of current. Due to the novel electronic structure and transport properties, single walled carbon nanotubes (SWCNTs) were found to be one of the promising candidates to satisfy this demand.<sup>6–10</sup> Up to now, there are in general three kinds of methods to achieve the spin polarization of current using SWCNTs, i.e., atomic or molecular doping,<sup>11–15</sup> connection with ferromagnetic (FM) electrodes,<sup>8,16,17</sup> and applying an external electric field.<sup>11,18–20</sup> However, these approaches are still challenging when the SWCNTs are integrated into the electronic circuit.

Recently, Sahin and Senger<sup>21</sup> proposed an all-carbon structure, i.e., graphene flakes contacted with electrode of carbon chain to produce the spin-polarized current. As is well known, finite-length open-ended SWCNTs can be considered as being rolled up from finite-length graphene nanoribbons (GNRs). The magnetisms of SWCNTs have been studied before<sup>11,22–27</sup> and it has been found that spin polarizations mainly occur at the edges. More interesting, these nanotubes exhibit half-metallic behavior by applying a limited range of external electric field.<sup>11,19</sup> On the other hand, Börnmert *et al.*<sup>28</sup> recently have made a breakthrough in preparing stable junctions between an SWCNT and a carbon atomic chain.<sup>29</sup> Then, we will naturally ask: can we avoid the use of the external electric field and explore these spin states with asymmetric contact method to manipulate the spin polarization of current? In the following, we will demonstrate that it is possible, but in a different mechanism.

For the graphene flake, the formation of spin-ordered edge-localized states along the zigzag edges is the key mechanism to generate the spin-polarized currents.<sup>21</sup> Previous studies showed that finite-length zigzag nanotubes also

have localized states at the edges.<sup>19,30</sup> In order to preserve these edge states and compare them with those of the graphene flake, we restrict ourselves to study zigzag nanotubes with different lengths and diameters. The paper is organized as follows: in Sec. II, we present our calculation methods. Geometrical structures, transport properties, and discussions, including the comparison with previous work are reported in Sec. III. At last, concluding remarks are given out in Sec. IV.

## II. CALCULATION METHODS

In present calculations, we use the carbon linear atomic chains as electrodes to strip off complications that may arise from electrode-tube interactions.<sup>21</sup> These chains are good candidates since they are metallic, and can make good contact with carbon nanotubes, and have atomically sharp tips.<sup>21</sup> More importantly, the whole system consists of carbon atoms only. The bond length in the linear chain is chosen as 1.27 Å.<sup>31</sup> Our calculations were carried out using the ATOMISTIX TOOLKIT package,<sup>32,33</sup> which is based on the combination of density functional theory (DFT) and nonequilibrium Green's function method. We used the mesh cutoff energy of 150 Ry, and  $1 \times 1 \times 50$   $k$ -point mesh in the Monkhorst–Pack scheme.<sup>34</sup> The Perdew–Burke–Eenzerhof<sup>35</sup> formulation of the generalized gradient approximation to the exchange–correlation functional was used. The double-zeta polarized basis set of local numerical orbitals was employed in all our calculations. The supercell with sufficient vacuum spaces (more than 10 Å) was chosen to prevent the interactions with adjacent images. To mimic the actual situation, the positions of all atoms and the distance between electrodes and the tube have been fully relaxed before the transport calculations. For the sake of clarity, the lengths of  $(n, 0)$  nanotubes are defined according to the number of carbon atoms along the tube axis, for example, L4, L6, etc.<sup>11</sup>

<sup>a)</sup>Electronic mail: xhyan@nuaa.edu.cn.

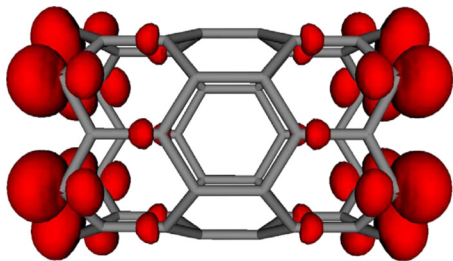


FIG. 1. (Color online) Geometry and spin charge density magnetization ( $\rho_{\uparrow} - \rho_{\downarrow}$ , the isovalue is  $8.69 \times 10^{-2} \text{ e}/\text{\AA}^3$ ) of L4-(6, 0) nanotube. Red (dark) and blue (light) represent positive and negative value, respectively. (Note that negative part is very small.)

### III. RESULTS AND DISCUSSIONS

We considered the two-probe geometry of carbon chain and nanotube with different diameter and length. The carbon nanotube under consideration with the minimum diameter is (6, 0) nanotube. The main reason why we choose (6, 0) tube is that the circumferential length is nearly the same as the width of graphene flake studied in Ref. 21. It will be very convenient to compare our results with those of graphene flakes. Figure 1 shows the atomic structure of L4-(6, 0) nanotube. It is a finite segment of (6, 0) nanotubes with 48 carbon atoms. Two ends of it are both zigzag patterns of carbon atoms. As the generations of spin-polarized currents are mainly related to electronic structures, the spin charge density magnetizations (i.e., up-spin charge density minus down-spin charge density) of our finite tube was shown in Fig. 1 (for clarity, balls for atoms were not shown). One can

see that, the magnetic charge density is mainly localized at the edge atoms. Also, the magnitudes of the density rapidly decay from the edge to the center of nanotube and become nearly zero in the middle region. So, the magnetic moments are actually arisen from zigzag edges, which is consistent with previous studies.<sup>11</sup> Based on the Mulliken analysis, we can obtain the magnetic moment of each atom, which can be regarded as another expression of spin charge density magnetization. The moments of carbon atoms in the zigzag edge rings are  $0.721 \mu_B$ . From the edges to the middle, the corresponding values of the second, third and fourth inner zigzag rings are  $0.023 \mu_B$ ,  $0.078 \mu_B$ , and  $0.011 \mu_B$ , respectively.

Now, we consider the L4-(6, 0) nanotube connected partially with atomic chains. We will discuss the spin-dependent transmission spectra and restrict our discussions to the condition of zero bias. For carbon chain and finite tube, there are six possible contact geometries for (6, 0) tube while only four are independent due to the symmetry, shown in Figs. 2(a)–2(d). In order to investigate the effect of electrode materials on transport properties, the spectrum of gold electrodes is also shown in Fig. 2(e) for comparison. From the results, one can see all transmission spectra are spin asymmetric. As for up-spin, the obvious difference among three cases can be found around the Fermi energy. In Figs. 2(a) and 2(d), there is one wide peak at  $-0.5 \text{ eV}$  (denoted by  $\alpha$ ), but in Figs. 2(b) and 2(c), it becomes a dip (denoted by  $\alpha'$ ). Through the transmission eigenchannel analysis, we found the depressions of one of two eigenchannels result in the dips

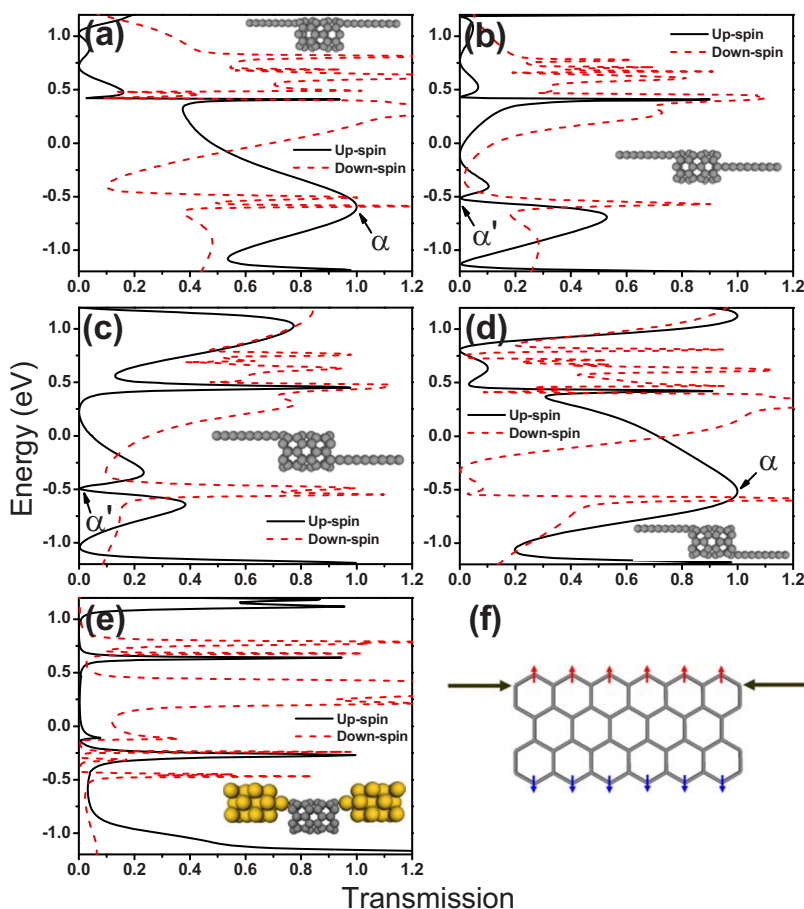


FIG. 2. (Color online) Spin-dependent transmission spectra of bare L4-(6, 0) nanotubes with four contact configurations with the leads, (a), (b), (c), and (d). (e) The lead in (a) is replaced by gold leads for up-spin (solid and black line) and down-spin (dashed and red line). (f) Schematic figure of graphene flake contacted with leads. (red/up arrow: up-spin and blue/down arrow: down-spin).

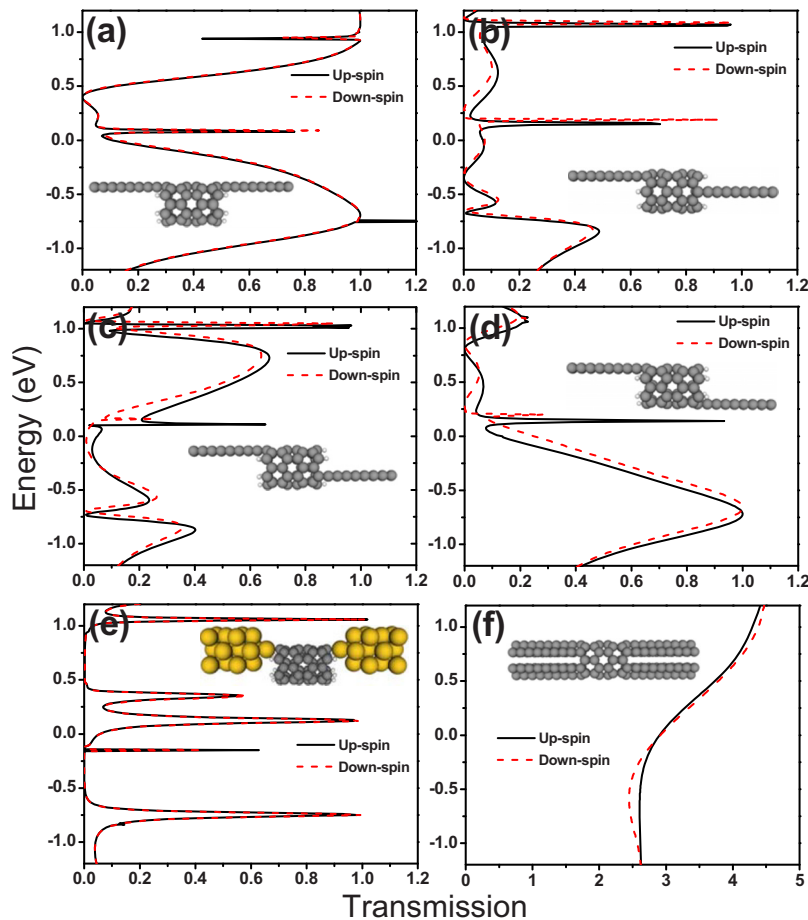


FIG. 3. (Color online) [(a)–(e)] The same as Figs. 2(a)–2(e) except that the nanotube is hydrogenated. (f) Spin-dependent transmission spectrum of L4-(6, 0) tube with uniformly contacted electrodes.

in (a) and (c) [from (a) to (d), the transmission eigenvalues of such an eigenchannel are 0.9988, 0.008852, 0.01140, and 0.9635, respectively]. Moreover, we would like to emphasize that for the case of the gold lead [Fig. 2(e)], the low transmission at  $-0.5$  eV is due to the weak coupling between carbon nanotube and gold electrodes.<sup>21</sup> For down-spin, many transmission peaks are present around 0.6 eV and one or two peaks are around  $-0.5$  eV. At the Fermi energy, they exhibit similar behavior. Moreover, the asymmetric features of transmission spectra exist even when the electrode is replaced by the gold wire. However, the transmission peaks are much fewer and narrower. Actually, these changes are due to the weak coupling between carbon nanotube and gold electrodes.<sup>21</sup>

Very interesting, when the edges of nanotube are saturated by hydrogen atoms, the situation is quite different. As shown in Figs. 3(a)–3(e), all spectra mentioned above become almost spin symmetric, although there are still some minor differences between up-spin and down-spin ones. In order to shed light on physical mechanism behind such a hydrogenation-induced-transition, we take the configuration in Figs. 2(a) and 3(a) as an example to demonstrate it. Figure 4 shows the spin charge density magnetizations for both bare and hydrogenated systems. For the bare one shown in Fig. 4(a), compared with the isolated tube (see Fig. 1), strong magnetization still exists, but the symmetry around the tube axis vanishes, especially at the contacts between electrodes and the tube, where the up-spin density was weakened while the down-spin one was enhanced. Due to the magnetization

and its asymmetric distribution, the scattering rates of transmitted electrons become spin asymmetric. Such behavior has been studied before in GNRs,<sup>36</sup> which indicates that symmetry plays an important role in the transport properties. After the tube was hydrogenated, the magnetization becomes very weak. The isovalue in Fig. 4(b) is  $1.231 \times 10^{-3} e/\text{\AA}^3$ , which is only one-tenth of that for the bare one in Fig. 4(a). For different spin electrons, the scattering are almost the same, and only some minor differences were induced by such a weak magnetization. One point should be noted that, the hydrogenation-induced-transition of transmission spectra from spin polarized to nonpolarized also takes place in the system with Au electrodes, which implies such a transition is an intrinsic feature of carbon nanotubes.

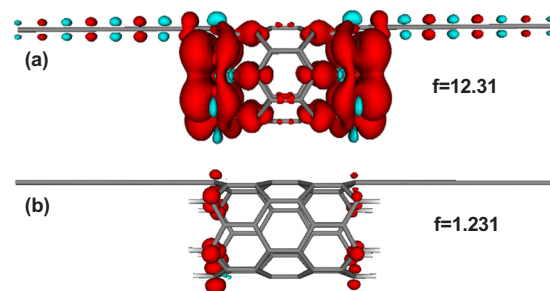


FIG. 4. (Color online) Geometry and spin charge density magnetization ( $\rho_{\uparrow} - \rho_{\downarrow}$ ) of bare (a) and hydrogenated and (b) L4-(6, 0) nanotubes contacted with carbon linear chains. Red (dark) and blue (light) represent positive and negative values, respectively. The isovalue of each plotted isosurface is  $f \times 10^{-3}$ , in units of  $e/\text{\AA}^3$ .

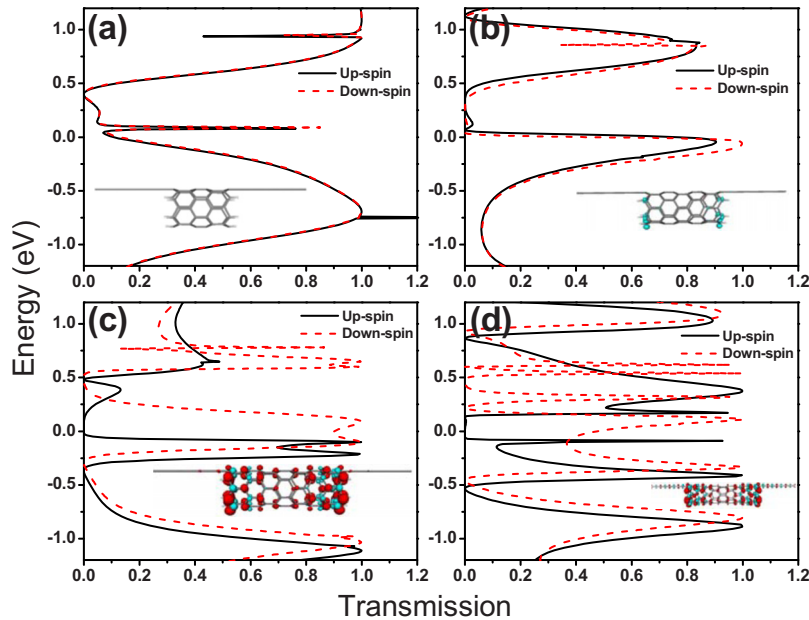


FIG. 5. (Color online) Spin-dependent transmission spectra of hydrogenated  $Lx-(6, 0)$  nanotubes with the same contact configuration as Fig. 2(a). Numbers  $x$  in (a), (b), (c), and (d) are 4, 6, 8, and 10, respectively. Insets are corresponding spin charge density magnetization with isosurface of  $1.231 \times 10^{-2} e/\text{\AA}^3$ .

In order to further demonstrate the partial contact is the key point to break spin symmetry, we carried out parallel calculations for  $L4-(6, 0)$  tube with uniformly contacted electrodes (contacted with 6 carbon chains at each edge). Its transmission spectrum is spin symmetric [see Fig. 3(f)], confirming our conclusions. In addition, compared with thinner electrodes, transmission probabilities of electrons for uniform contact are much higher. This is due to the increased number of conduction channels induced by wider electrodes.

From above results, we conclude that, spin-polarized currents can easily be achieved by the bare finite zigzag tube partially contacted with carbon chain electrodes. Some additional calculations for bare tubes with various lengths, diameters and connection configurations were also performed (the results are not shown), and we got the same conclusion. Although spin-polarized currents can be achieved by bare tubes, but the DFT calculations predict that hydrogenated tubes are more stable. The high stability will be important and essential for practical applications. Hence, we next will

search for possible ways to obtain spin-polarized currents in hydrogenated nanotubes by changing the size of nanotubes.

As the transmission spectrum of hydrogenated  $L4-(6, 0)$  tube has been proved to be spin symmetric, we will turn to the tubes with different lengths and diameters. We next discuss the effect of tube length on the transmission spectrum shown in Fig. 5. When the hydrogenated tube becomes longer, a separation of up-spin and down-spin spectra becomes clearer and clearer. Although hydrogenation will induce spin depolarization, even almost nonpolarization for  $L4-(6, 0)$  tube, this effect becomes weaker as the tube becomes longer. A good benefit brought from the spin separation is that, in some energy regions, especially around the Fermi energy, a complete spin polarization of the spectrum can be obtained. In order to show it more clearly, we plot the energy-dependent relative spin polarization of the transmission probabilities,<sup>21</sup>  $(T_{\text{up}} - T_{\text{down}})/(T_{\text{up}} + T_{\text{down}})$ , in Fig. 6. It is another view of Fig. 5. For hydrogenated  $L8-(6, 0)$  [Fig. 5(c)] and  $L10-(6, 0)$  [Fig. 5(d)] tubes, complete polarizations

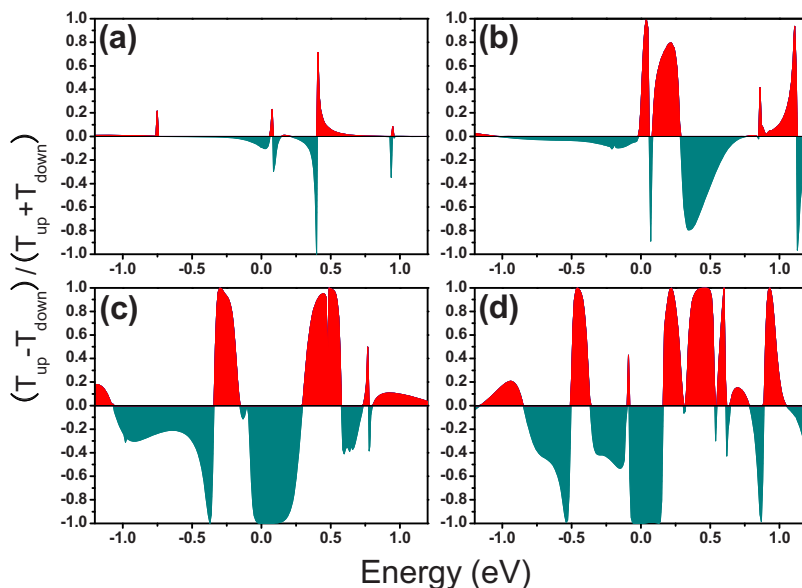


FIG. 6. (Color online) Spin polarization in the transmission spectra for systems in Fig. 5. Red (dark) and blue (light) represent positive and negative values, respectively.

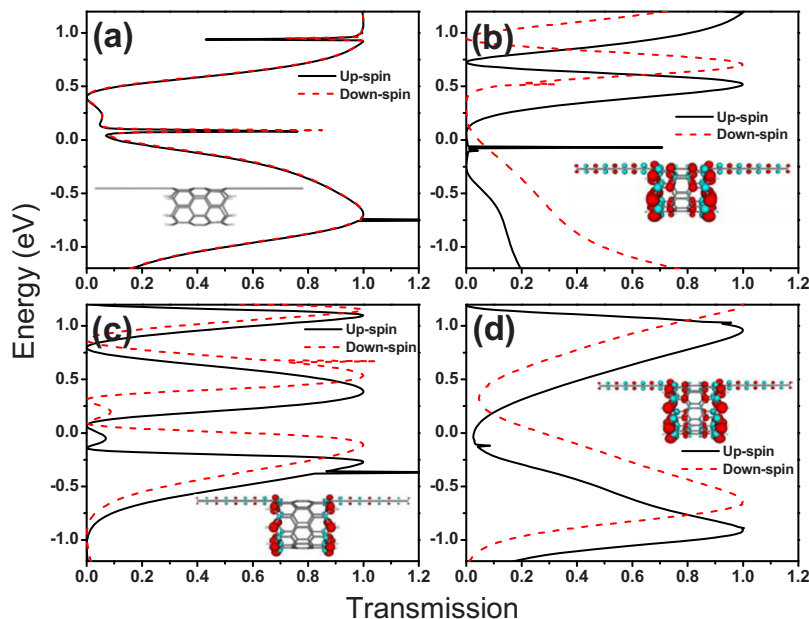


FIG. 7. (Color online) Spin-dependent transmission spectra of hydrogenated L4-( $n$ , 0) nanotubes with the same contact configuration as Fig. 2(a). Numbers  $n$  in (a), (b), (c), and (d) are 6, 7, 8 and 9, respectively. Insets are corresponding spin charge density magnetization with isosurface of  $1.231 \times 10^{-2} e/\text{\AA}^3$ .

occur in an energy window around the Fermi level. As is known, a high or nearly complete polarization is quite essential for the development of spintronic devices. Du *et al.* have showed that, finite-length hydrogenated zigzag nanotubes can display half metallicity, but only under a limited range of external electric field.<sup>11,19</sup> However, our results give an explicit way to realize it by linking a nanotube to carbon chains, instead of using the external electric field. Also, complete spin-polarized currents can be produced, providing an option for spintronic devices.

Figure 7 shows the effect of tube diameter on the transmission spectrum. Again, we observe the separations of transmission spectra for up-spin and down-spin. Du *et al.* found that,<sup>11</sup> as the diameter of the SWCNT increases, all finite-length ( $n$ , 0) nanotubes become magnetic and the AFM phase appears to be the ground state for large diameter nanotubes. This is exactly consistent with our results, except for L4-(6, 0) tube, i.e., the spin separations take place in all other three cases through the contact with carbon chain electrodes.

So, we conclude that, a special and partial contact can play the same role as the external electric field in manipulating the spin dependent transport. Another important point is that, for each of the spectra, we can clearly see a relative spectrum shift between up-spin and down-spin along the energy axis. Figure 8 shows  $(T_{\text{up}} - T_{\text{down}})/(T_{\text{up}} + T_{\text{down}})$  for these four cases. In Figs. 8(b)–8(d), each spin polarization at least exceeds 80% in the energy window around the Fermi level, which may be very useful for spintronic devices.

As a result, the transmission spectra for hydrogenated nanotubes become spin asymmetric as the diameter and length are increasing. In order to understand it, we plot spin charge density magnetization ( $\rho_{\uparrow} - \rho_{\downarrow}$ ) for each case (see the insets of Figs. 5 and 7). As is seen, the magnetic moments, especially at the zigzag edges, increase with the length and diameter, which finally results in a pronounced spin polarization. When the large spin polarization is present, the transmission probability of up or down-spin electrons will be

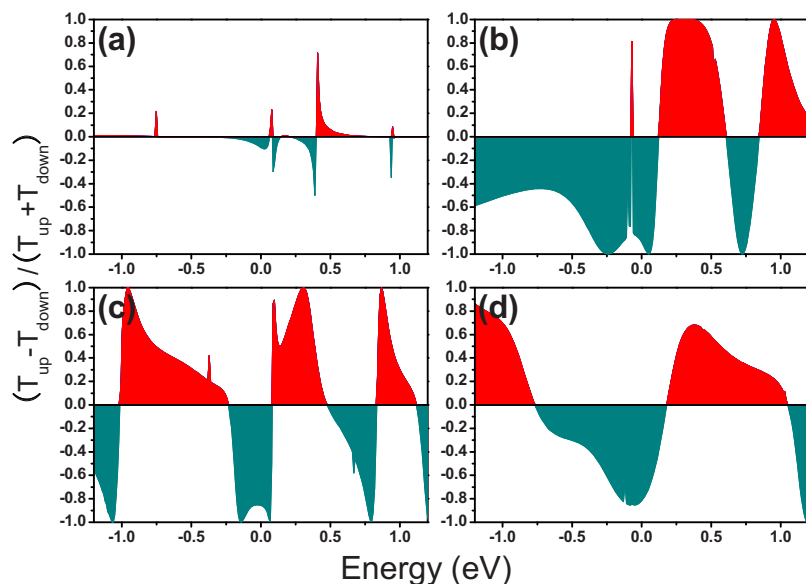


FIG. 8. (Color online) Spin polarization in the transmission spectra for systems in Fig. 7. Red (dark) and blue (light) represent positive and negative values, respectively.

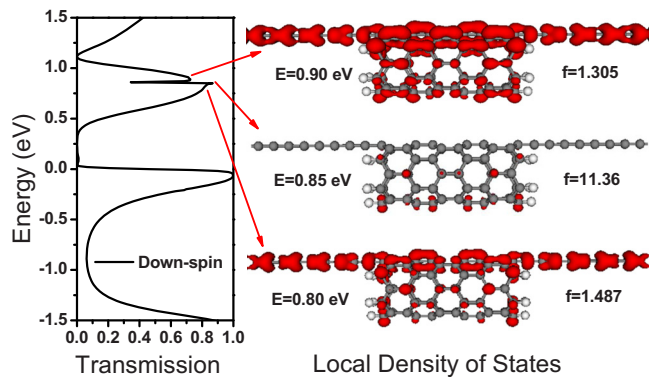


FIG. 9. (Color online) LDOS isosurfaces calculated for particular energies of the down-spin transmission spectrum of partially contacted L6-(6, 0) tube. The isovalue of each plotted LDOS isosurface is  $f \times 10^{-2}$ , in units of states/ $\text{\AA}^3$  eV.

different, thereby inducing the spin asymmetry in transmission spectra.

In the above, we have presented many transmission spectra. Among them, we notice that there are some discontinuities in the curves. These features also appear in the transmission spectra of graphene flake and often in the form of a rapid variation with very narrow dips and adjacent peaks.<sup>21</sup> They were also found in some other transport systems<sup>12</sup> and were usually explained by the coupling between localized states of a quantum dot and continuous states of a quantum channel.<sup>21,37</sup> Furthermore, they can be regarded as the traces of Fano resonances. In our system, the finite tubes play a role of quantum dot and the electrodes act like the quantum channel. Figure 9 gives us a clear understanding about it, in which the local density of states (LDOS) for down-spin of hydrogenated L6-(6, 0) was shown. In the transmission spectrum, there is a resonance located at about 0.85 eV. We plot the three-dimensional LDOS isosurfaces for three energies, 0.90 eV, 0.85 eV and 0.80 eV (see right panel of Fig. 9). Obviously, only at resonance energy, i.e., 0.85 eV, the LDOS was almost confined inside the finite tube region. At the other two off-resonance energies, the extended states of electrodes dominate the LDOS.

Last, we will compare our results with those of graphene flake.<sup>21</sup> In order to show it clearly, we plot a schematic figure of graphene flake contacted with leads in Fig. 2(f) (red/up arrow: up-spin and blue/down arrow: down-spin). The difference of electronic transmission behavior between GNR and carbon nanotube is arisen from the contact geometry. The largest difference of contact geometry is the edges contacted by the lead for two carbon structures. We take a zigzag nanoribbon for example to show how the edges affect the electronic transport. For zigzag nanoribbon, there are two zigzag edges (top and bottom), which play important role in the electronic transport of nanoribbon.<sup>21</sup> These two zigzag edges are parallel to carbon chains. If carbon chains contact with the same zigzag edge [see Fig. 2(f)], the transmission probabilities of electrons with the spin which dominate at this edge will increase, while another one will be suppressed. As an example, in Fig. 2(f), the up-spin electrons dominate in the top zigzag edge. So, the transmission probability of up-spin electrons will be larger than that of down-spin ones and

then the current becomes spin-polarized. When both up-spin and down-spin edges contact with the electrodes, there is no dominating spin, and the transmission will be spin-unpolarized.<sup>21</sup> However, for our systems, the zigzag edges of nanotube (left or right) are perpendicular to the electrodes, so the electrodes always contact with two different zigzag edges (see Fig. 5 or 7). At the edges [e.g., Fig. 5(c)], the magnetization and its distribution become asymmetric due to the interaction between electrodes and tube, which finally results in the spin polarization and spin asymmetry in transmission spectra.

Recently, Qin *et al.*<sup>38</sup> have studied the magnetoresistance ratio (MR) of zigzag-edged GNR (ZGNR). They found that the MR of nonhydrogenated ZGNRs is one to five orders of magnitude higher than that of hydrogenated ones. This behavior is partially attributed to the significantly enhanced exchange splitting by the dangling bond.<sup>38</sup> Based on similar dangling bonds in our system, we expect that a similar enhancement in MR may appear for carbon nanotube-chain system.

#### IV. CONCLUSION

In summary, we have performed *ab initio* calculations of transmission spectra for finite-length carbon nanotubes. For bare nanotubes, spin-polarized currents can be always obtained by partial contact between the tube and electrodes, i.e., carbon atomic chains. For hydrogenated nanotubes, in the same geometrical configuration, only nanotubes longer or wider than L4-(6, 0) can achieve the spin polarization current. Especially, in several cases, e.g., L8-(6, 0) and L10-(6, 0), the 100% polarizations have been obtained, which is essential for spintronic devices. As there is no dopant, FM electrodes, and external electric field, it is another way to produce the spin-polarized current with the system proposed here. Moreover, the traces of Fano resonances are found in the spectra. Our results will be of significant importance for future spintronic applications.

#### ACKNOWLEDGMENTS

We would like to thank Professor Z. Zeng for academic help. This work was supported by the National Natural Science Foundation of China (Grant Nos. 10874089 and 51032002) and partly by the Natural Science Foundation of Jiangsu Province of China (Grant No. BK2008398). Y.X. would like to acknowledge the support from China Postdoctoral Science Foundation Funded Project (Grant No. 20090461114) and Jiangsu Planned Projects for Postdoctoral Research Funds (Grant No. 0902093C).

<sup>1</sup>S. Wolf, D. Awschalom, R. Buhrman, J. Daughton, S. Von Molnar, M. Roukes, A. Chtchelkanova, and D. Treger, *Science* **294**, 1488 (2001).

<sup>2</sup>I. Zutic, J. Fabian, and S. Das Sarma, *Rev. Mod. Phys.* **76**, 323 (2004).

<sup>3</sup>D. Awschalom and M. Flatté, *Nat. Phys.* **3**, 153 (2007).

<sup>4</sup>A. Fert, *Rev. Mod. Phys.* **80**, 1517 (2008).

<sup>5</sup>N. Poli, J. P. Morten, M. Urech, A. Brataas, D. B. Haviland, and V. Korenivski, *Phys. Rev. Lett.* **100**, 136601 (2008).

<sup>6</sup>J. Fürst, J. Hashemi, T. Markussen, M. Brandbyge, A. Jauho, and R. Nieminen, *Phys. Rev. B* **80**, 035427 (2009).

<sup>7</sup>S. Ciraci, S. Dag, T. Yildirim, O. Gulseren, and R. T. Senger, *J. Phys.: Condens. Matter* **16**, R901 (2004).

- <sup>8</sup>A. Cottet, T. Kontos, S. Sahoo, H. Man, M. Choi, W. Belzig, C. Bruder, A. Morpurgo, and C. Schönenberger, *Semicond. Sci. Technol.* **21**, S78 (2006).
- <sup>9</sup>A. Brataas, *Nature (London)* **452**, 419 (2008).
- <sup>10</sup>F. Kuemmeth, S. Ilani, D. C. Ralph, and P. L. McEuen, *Nature (London)* **452**, 448 (2008).
- <sup>11</sup>A. Du, Y. Chen, G. Lu, and S. Smith, *Appl. Phys. Lett.* **93**, 073101 (2008).
- <sup>12</sup>J. Fürst, M. Brandbyge, A. Jauho, and K. Stokbro, *Phys. Rev. B* **78**, 195405 (2008).
- <sup>13</sup>C. Yang, J. Zhao, and J. Lu, *Nano Lett.* **4**, 561 (2004).
- <sup>14</sup>C.-K. Yang, J. Zhao, and J. P. Lu, *Phys. Rev. Lett.* **90**, 257203 (2003).
- <sup>15</sup>X. Q. Shi, Z. X. Dai, G. H. Zhong, X. H. Zheng, and Z. Zeng, *J. Phys. Chem. C* **111**, 10130 (2007).
- <sup>16</sup>C. Schenke, S. Koller, L. Mayrhofer, and M. Grifoni, *Phys. Rev. B* **80**, 035412 (2009).
- <sup>17</sup>H. T. Man, I. J. W. Wever, and A. F. Morpurgo, *Phys. Rev. B* **73**, 241401 (2006).
- <sup>18</sup>S. Sahoo, T. Kontos, J. Furer, C. Hoffmann, M. Graber, A. Cottet, and C. Schonenberger, *Nat. Phys.* **1**, 99 (2005).
- <sup>19</sup>A. Mañanes, F. Duque, A. Ayuela, M. López, and J. Alonso, *Phys. Rev. B* **78**, 035432 (2008).
- <sup>20</sup>Y. Son, J. Ihm, M. Cohen, S. Louie, and H. Choi, *Phys. Rev. Lett.* **95**, 216602 (2005).
- <sup>21</sup>H. Şahin and R. T. Senger, *Phys. Rev. B* **78**, 205423 (2008).
- <sup>22</sup>H. Şahin, C. Ataca, and S. Ciraci, *Appl. Phys. Lett.* **95**, 222510 (2009).
- <sup>23</sup>H. Şahin, C. Ataca, and S. Ciraci, *Phys. Rev. B* **81**, 205417 (2010).
- <sup>24</sup>Y.-H. Kim, J. Choi, K. J. Chang, and D. Tománek, *Phys. Rev. B* **68**, 125420 (2003).
- <sup>25</sup>S. Okada and A. Oshiyama, *J. Phys. Soc. Jpn.* **72**, 1510 (2003).
- <sup>26</sup>N. Park, M. Yoon, S. Berber, J. Ihm, E. Osawa, and D. Tománek, *Phys. Rev. Lett.* **91**, 237204 (2003).
- <sup>27</sup>D. Huertas-Hernando, F. Guinea, and A. Brataas, *Phys. Rev. Lett.* **103**, 146801 (2009).
- <sup>28</sup>F. Börrnert, C. Börrnert, S. Gorantla, X. J. Liu, A. Bachmatiuk, J. O. Joswig, F. R. Wagner, F. Schäffel, J. H. Warner, R. Schönfelder, B. Relinghaus, T. Gemming, J. Thomas, M. Knupfer, B. Büchner, and M. H. Rummeli, *Phys. Rev. B* **81**, 085439 (2010).
- <sup>29</sup>K. H. Khoo, J. B. Neaton, Y. W. Son, M. L. Cohen, and S. G. Louie, *Nano Lett.* **8**, 2900 (2008).
- <sup>30</sup>Z. Y. Zhou, M. Steigerwald, M. Hybertsen, L. Brus, and R. A. Friesner, *J. Am. Chem. Soc.* **126**, 3597 (2004).
- <sup>31</sup>S. Tongay, R. T. Senger, S. Dag, and S. Ciraci, *Phys. Rev. Lett.* **93**, 136404 (2004).
- <sup>32</sup>M. Brandbyge, J.-L. Mozos, P. Ordejón, J. Taylor, and K. Stokbro, *Phys. Rev. B* **65**, 165401 (2002).
- <sup>33</sup>J. Taylor, H. Guo, and J. Wang, *Phys. Rev. B* **63**, 245407 (2001).
- <sup>34</sup>H. J. Monkhorst and J. D. Pack, *Phys. Rev. B* **13**, 5188 (1976).
- <sup>35</sup>J. P. Perdew, K. Burke, and M. Ernzerhof, *Phys. Rev. Lett.* **77**, 3865 (1996).
- <sup>36</sup>Z. Y. Li, H. Y. Qian, J. Wu, B. L. Gu, and W. H. Duan, *Phys. Rev. Lett.* **100**, 206802 (2008).
- <sup>37</sup>H. Xu and W. Sheng, *Phys. Rev. B* **57**, 11903 (1998).
- <sup>38</sup>R. Qin, J. Lu, L. Lai, J. Zhou, H. Li, Q. Liu, G. Luo, L. Zhao, Z. Gao, and W. Mei, *Phys. Rev. B* **81**, 233403 (2010).